

CFD-ASSISTED REGENERATOR ANALYSIS: APPLICATION TO THERMOACOUSTIC SYSTEM

SAAT F. A. Z., YU Z., JAWORSKI A. J.

School of Mechanical, Aerospace and Civil Engineering,
University of Manchester, Sackville Street, P.O. Box 88,
Manchester M60 1QD, United Kingdom.
a.jaworski@yahoo.co.uk

ABSTRACT

Thermoacoustic devices have been of considerable research interest in the last few decades due to their simplicity and the environmentally friendly operation. This paper investigates the regenerator, forming the core of a thermoacoustic device, where the thermoacoustic effect takes place. A two-dimensional axis-symmetrical computational fluid dynamic (CFD) model of a thermoacoustic effect in a travelling-wave case has been developed. The boundary conditions were imposed according to the measured oscillating pressure and the temperature gradient developed across the regenerator in a thermoacoustic test rig. The simulation was validated by comparing the resulting pressure with that measured experimentally at a number of locations. A friction factor correlation was derived for the CFD-assisted model and compared with the experimental data available.

1. INTRODUCTION

Regenerators in the thermoacoustic systems are often constructed out of a porous medium. Here the thermoacoustic effect results from a complex heat transfer interaction between the sound wave (an oscillatory compressible flow) and the solid body (the porous/tortuous medium). The typical design issue is that whilst the porous/tortuous structure offers a good thermal contact between the solid and gas, the pressure drop and inertial losses could degrade the overall performance of the system. In the pursuit of an efficient thermoacoustic system, finding and understanding the causes of performance degradation is of utmost importance.

The regenerators used in the thermoacoustic devices are commonly built from stacks of screen mesh. The screen mesh with a very fine wire diameter is stacked randomly creating a porous structure. The correct characteristic of such media is important to help optimise the performance of the whole system. In the numerical analysis, the regenerator is commonly modelled using a porous medium theory. Modelling a momentum transfer in porous media requires determination of the important characteristic parameters related to it, namely the Darcy permeability, K , Forchheimer inertial coefficient, F , and the Brinkmann number. The appropriate form of Darcy-Forchheimer model is presented as pressure gradient, ∇p , and written as (Bejan et. al., 2003);

$$\nabla p = -\frac{\mu}{K} \mathbf{v} - FK^{-1/2} \rho |\mathbf{v}| \mathbf{v} \quad (1)$$

where μ , ρ , and \mathbf{v} are the gas dynamic viscosity, density and velocity, respectively. In the simplest case, the flow across the porous medium can be represented by Darcy's law. This law is valid only when the Reynolds number, defined by the average flow velocity, is in an order of magnitude smaller than one. Darcy's law simply neglects the second term on the right hand side of eq. (1). When the velocity is higher, the Forchheimer modified equation should be considered to account for the inertial losses in the porous medium. This is exactly the case presented by eq. (1). In a highly viscous flow, a further modification should be considered by replacing the second term on the right hand side of eq. (1) with the Brinkmann number, $(K\nabla^2 \mathbf{v})$.

Darcy's Permeability, K , and Forchheimer Inertial Coefficients, F , are empirical constants. As empirical constants, both permeability and inertial coefficients are uniquely dependent on the porosity and tortuosity of the porous structure. The values will determine the momentum losses occurring in the porous media. The momentum loss can be experimentally measured by the pressure drop across the porous region.

Cha et. al. (2008) reported a CFD-assisted method for determining the permeability and inertial coefficient of a porous regenerator in an oscillating flow. The regenerator in their study, limited to a few mesh numbers, was tested in a small size device where the inertial effect could be significant. These coefficients were also derived by Tao et. al. (2009). In the derivation, an oscillating flow friction factor reported by Nam and Jeong (2006) was used. The pressure drop resulting from their numerical simulation deviated quantitatively from the experimental result. The reason for this was not reported. The derived equation was not generalised as the friction factor used in defining the pressure drop was the specific cryogenic condition equation.

CFD approach has been used extensively to model several other thermoacoustic phenomena including a stack of a standing wave system and a pulse tube cooler (cf. Ashwin et. al., 2010, Yu G. et. al., 2010). The present CFD-assisted study focuses on two aspects. Firstly, the friction factor of the porous media is presented as a function of permeability coefficient and Reynolds number based on the hydraulic radius. This is important when comparing a numerical model with the experimental friction factor as most of the friction factor equations in experimental studies are presented as a Reynolds number based on the hydraulic radius. Secondly, the regenerators tested in the present study were subjected to the travelling-wave conditions.

The difference between the travelling-wave and standing-wave time phasing between pressure and velocity oscillations could influence the permeability and inertial coefficients of the regenerator. Hsu (2005) showed that when a phase difference exists, setting the amplitude alone was not sufficient to predict the hydrodynamics of flow in the porous medium. The theoretical prediction in that study was in good agreement with experimental result when the phasing was considered. In thermoacoustic applications, the regenerators work typically in a travelling-wave mode and hence it is very important to predict the porous coefficients using the correct time phasing. In the current study, both the experiment and simulation were carefully conducted in an arrangement with the travelling-wave time phasing between pressure and velocity.

2. THEORETICAL MODEL

The hydrodynamic characteristics of the experimental and simulation models are presented using a dimensionless parameter known as friction factor. For an oscillatory flow, the friction factor is defined using the amplitude of pressure drop and the velocity amplitude as given by Choi et. al. (2004);

$$f_{osc} = \frac{X_{\Delta p} d_h}{2\rho X_{um}^2 L_r} \quad (2)$$

Eq. (2) is based on Fanning friction factor which is related to Darcy friction factor, f , by $f=4f_{osc}$. The amplitude of pressure drop, $X_{\Delta p}$, and mean velocity, X_{um} , were measured experimentally in an oscillatory situation; ρ , is the fluid density and L_r is the length of the regenerator. The hydraulic diameter, d_h , is defined as $d_h=\phi d_w/(1-\phi)$. The value of porosity, ϕ , and the wire diameter, d_w are usually supplied by the manufacturer/supplier. The experimental friction factor was fitted to obtain a representative experimental correlation. A few models of correlations are discussed here.

Friction factor can be modelled in the standard two-parameter Ergun form (Gedeon and Wood, 1996);

$$f = \frac{a_1}{\text{Re}} + a_2 \quad (3)$$

where a_1 and a_2 are to be determined. Several modifications were found in the literature in an effort to find a better definition for the oscillating flow condition. Gedeon and Wood (1996) introduced a three-parameter-Ergun correlation. Swift and Ward (1996) represented a friction factor in a standard Ergun equation form with a new definition of the coefficients a_1 and a_2 in terms of porosity.

Another modification was also proposed in the literature where the Ergun-form correlation was multiplied by a certain parameter and had the modified form shown to be $f=a_0^{-1}[(a_1/\text{Re})-a_2]$. In the study of Ju (1998), for example, a dimensionless distance, $X_d=u_{max}/(2d_h\omega)$, was introduced as a_0 . Nam and Jeong (2005) defined a_0 as breathing factor, B , introduced as $B=X_{\Delta m}RT_m/L_rA_g\omega X_{pm}$. Nam and Jeong (2005) included the breathing factor in their correlation for a precise estimation of the phase angle of the pressure drop and the mass flow rate in regenerators. The breathing factor included the effect of the gas constant (R), the mean temperature (T_m), the cross sectional area of regenerator (A_g), the angular frequency (ω), the amplitude of mass flow rate ($X_{\Delta m}$), and the amplitude of mean pressure, (X_{pm}). In a separate research paper, Nam and Jeong (2006) further investigated the validity of their correlation at cryogenic operation temperatures. A new friction factor correlation was suggested to include the Valensi number, Va , and expansion parameter, ε . In all the literature discussed above, the Reynolds number for the flow across regenerator was defined using the hydraulic radius as given by Swift and Ward (1996);

$$\text{Re}_h = \frac{4u_1r_h\rho_m}{\mu} = \frac{\rho_mu_1d_h}{\mu} \quad (4)$$

where u_1 is the first order spatial average velocity and the hydraulic diameter, d_h , is 4 times the hydraulic radius, r_h .

In porous medium theory, the friction factor of most porous media is presented by the permeability Reynolds number, $\text{Re}_K = \rho u K^{1/2}/\mu$. The pressure gradient is given by Bejan et. al. (2003);

$$-\nabla P = \frac{1}{2} \frac{f\rho v^2}{\sqrt{K}} \quad (5)$$

The pressure gradient can also be presented by Darcy-Forchheimer model as in eq. (1). The following formula can be derived from eq. (1) and eq. (5);

$$f = \frac{2\sqrt{K}}{\rho u^2} \left[\frac{\mu}{K} u + \frac{F\rho}{\sqrt{K}} u^2 \right] \quad (6)$$

Further modification can be made to include the hydraulic radius term:

$$f = \frac{2\sqrt{K}}{\rho u^2} \cdot \frac{d_h}{d_h} \left[\frac{\mu}{K} u + \frac{F\rho}{\sqrt{K}} u^2 \right] \quad (7)$$

$$f = \frac{2d_h}{\sqrt{K}} \cdot \frac{1}{\text{Re}_h} + 2F \quad (8)$$

The permeability coefficient, K , has a unit $(\text{length})^2$, while Forchheimer inertial coefficient, F , is dimensionless. Simple dimensional analysis shows that eq. (8) is dimensionless. Interestingly, the friction factor derived is still following the well-known Ergun form presented in eq. (3). From this derived friction factor, the coefficients a_1 and a_2 in the Ergun equation are defined as;

$$a_1 = \frac{2d_h}{\sqrt{K}} \quad ; \quad a_2 = 2F \quad (9)$$

In the simplest Darcy model, the inertia effects can be neglected and the friction factor is left with;

$$f = \frac{2d_h}{\sqrt{K}} \cdot \frac{1}{\text{Re}_h} \quad (10)$$

With this correlation, the porous coefficient predicted through CFD-assisted method can be used to predict the friction factor of the porous medium and then compared to the experimentally calculated friction factor.

3. EXPERIMENTAL SETUP

The schematic diagram of the travelling wave test rig is shown in Figure 1. The rig consists of a linear motor, resonator, hot and cold heat exchanger, regenerator and the resistance, inductance, compliance network (RLC). The frequency of the acoustic wave was set using an acoustic driver connected to a linear motor. The linear motor was enclosed in a specially designed high pressure cylinder with a specially designed glass window to allow a laser displacement measurement of the motor piston. The laser displacement sensor (Keyence LK-G152) sensed the piston displacement, δ . The velocity amplitude was then calculated as $u=\omega\delta$.

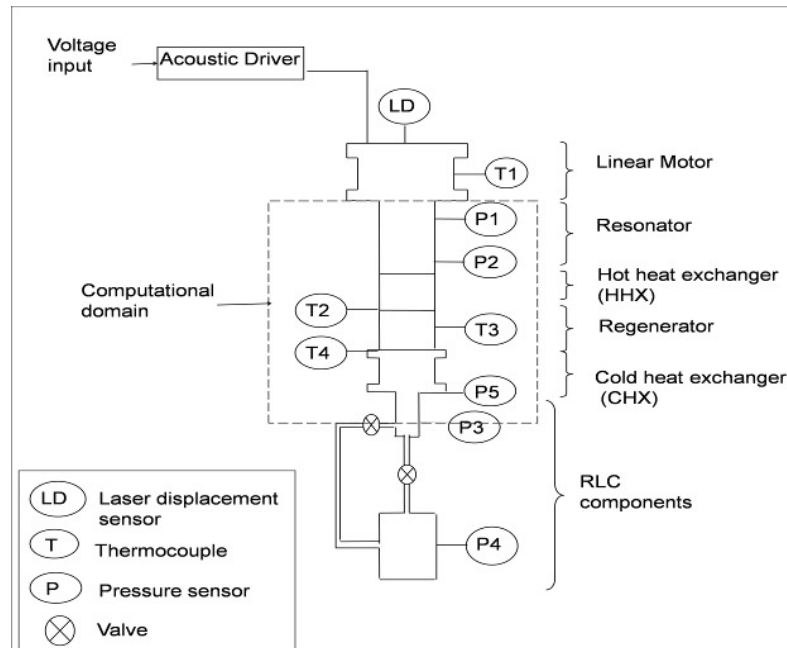


Figure 1: Schematic representation of the experimental rig and the selected computational domain.

The resonator, hot heat exchanger, regenerator and cold heat exchanger shared the same inner diameter of 55 mm while the lengths were 185 mm, 25 mm, 50 mm and 27 mm respectively. The acoustic wave supplied created a temperature gradient along the regenerator. Temperatures, at location T1, T2, T3 and T4, were measured by type-K thermocouples. Table 1 gives the details of each regenerator sample tested.

Table 1: Geometric dimension of regenerator tested.

Mesh screen regenerator (material: stainless steel)				
Regenerator	Mesh number	Wire diameter (mm)	Porosity (%)	Hydraulic radius (μm)
1	180	0.058	67.5	30.31
2	200	0.041	74.8	30.27
3	30	0.28	72.7	195
4	94	0.089	74.2	63.79

The travelling-wave time phasing was controlled via the RLC network, designed as a combination of suitable valves, a 1.6 m long tube with diameter of 8 mm and a buffer volume ($2.5 \times 10^{-3} \text{ m}^3$). The valve was adjusted accordingly until the travelling-wave phase was achieved. Four differential pressure transducers (PCB#112A21), connected to a signal conditioner (PCB Piezotronics 480B21), were used to measure the transient gas pressure wave at locations P1, P2, P3, P4 and P5. Data was collected using a PC-based data acquisition board. The time phasing was monitored and carefully calculated to ensure that a near travelling-wave phasing was achieved in every test. The friction factor was calculated from the experimental results using eq. (2).

4. COMPUTATIONAL SETUP

The computational model (Figure 2) is a two-dimensional axis-symmetrical model. The model was solved according to the flow characteristics in the domain. Flow in the domain filled by the regenerator was solved using porous medium theory. Elsewhere, the flow and energy transfer was solved using standard flow and energy equation available in Fluent 6.3. In general the equations can be simplified as follows;

$$\frac{\partial \rho}{\partial t} + \nabla \cdot (\rho \vec{v}) = 0 \quad (11)$$

$$\frac{\partial}{\partial t} (\rho \vec{v}) + \nabla \cdot (\rho \vec{v} \vec{v}) = -\nabla p + \nabla \cdot (\tau) + \rho \vec{g} + \vec{F} \quad (12)$$

$$\frac{\partial}{\partial t} (\rho E) + \nabla \cdot (\vec{v} (\rho E + p)) = \nabla \cdot (k_{eff} \nabla T + \tau \cdot \vec{v}) \quad (13)$$

For the porous medium region, an additional term was added in the momentum equation to count for the losses due to the presence of the porous media. The additional term was defined as $S = -D_x \mu v_x + (C_x \rho v v_x)/2$. The accuracy of the solution for the porous medium flows was improved by applying a physical velocity throughout the porous flow field. The relationship between Fluent's tensor (D_x and C_x) and the real Darcy permeability, K , and Forchheimer initial coefficients, F , as presented in porous medium equation were given by;

$$K = \frac{\phi^2}{D_x} \quad ; \quad F = \frac{C_x \sqrt{K}}{2\phi^3} \quad (14)$$

In this study, the porous medium is treated as isotropic where the radial loss was small and negligible. Furthermore, the velocity in the cases investigated was low. Therefore, the inertial effect was also negligible. In the most general thermoacoustic theory, all dependent variables are treated as a simple harmonic oscillating flow. These variables are expressed in terms of mean components and first order fluctuating components, except for velocity where the mean component is zero. The higher order part of the fluctuation is commonly very small and negligible (Swift, 1996). This simple harmonic equation is used appropriately, when defining the boundary conditions in Fluent.

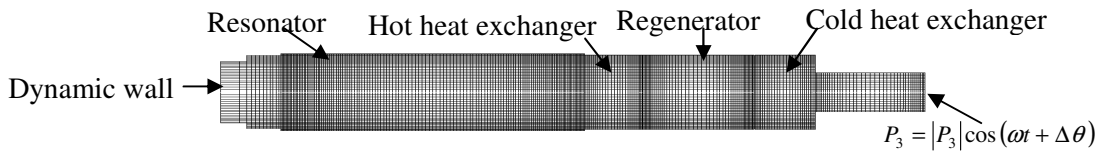


Figure 2: Computational domain for the regenerator study using the travelling-wave test rig.

A dynamic meshing was imposed as the inlet boundary condition to replicate the movement of the piston in the linear motor. The space between the dynamic mesh area and resonator was a short tube (15 mm in length and 50 mm in diameter). The computational domain excluded the RLC network, but imposed the phase control using a user defined function (UDF) at the inlet wall and the exit pressure at location P3 (refer to Figure 1). The last region after the cold heat exchanger was 75.5 mm long and had a diameter of 27.17 mm. The working gas was set as ideal gas equation, which allowed for temperature and pressure dependent variations of the gas density. The regenerator was set as a porous medium. The porous medium transport equation with a thermal equilibrium assumption was solved for the flow and energy transfer across the regenerator. The model was solved using an unsteady pressure-based implicit solver with the first order implicit scheme for the discretization of time. Pressure-velocity coupling was solved using PISO algorithm available in Fluent. The discretization for all variables (pressure, density, momentum and energy) is second-order upwind.

The simulation model was also tested for grid independency. The grid was developed to be denser near the wall and at the interface between the resonator, heat exchanger and regenerator. The mesh at the inlet was made coarser to allow for the movement of the inlet wall. The grid independency test was carried out by increasing the number of mesh points by a factor of 1.3. The grid structure was kept the same and only the mesh density was increased. The model was also run in both single and double precision solver to test for round-off error. It appeared that the single precision was sufficient to solve this 2D axis-symmetrical model.

The operating pressure was set at 25 bars. The hot and cold heat exchangers were also set as porous media with their characteristics following Cha (2008). Temperatures of the hot and cold heat exchangers were set following the measured temperatures in the experimental run. The temperature developed was the result of the thermoacoustic effect occurring at the regenerator according to the travelling-wave time phasing. In the simulations, the hot heat exchanger was set at a constant temperature. This is consistent with the experiments where the data was collected only after the temperatures at the hot and cold heat exchangers were constant.

5. CFD MODEL VALIDATION

The simulation model was pre-validated after setting the appropriate boundary conditions and the solver. At this stage, only the velocity and pressure at the location before the porous medium were compared to the experiment. The permeability coefficient of the regenerator was then predicted by carefully increasing the Fluent's permeability value until the pressure drop matched the experiment value. Once the pressure drop matched, the validation was finalised by comparing the inlet velocity (V1 in Figure 3) and pressure at location P2 and P5 (refer to Figure 1). The same procedure was repeated for each case until a good agreement with experiment was obtained. All four regenerator models were validated but only one case is presented here.

Simulated pressure was compared to the experimentally measured value. The inlet velocity was validated using the calculated velocity from the displacement measurement at the inlet location. Figure 3 confirms that the pressure and velocity near the inlet was not in-phase due to the movement of the displacer of the linear motor, as measured in the experiment. The time-phasing between pressure and velocity at the regenerator reached the travelling-wave phasing due to the RLC control.

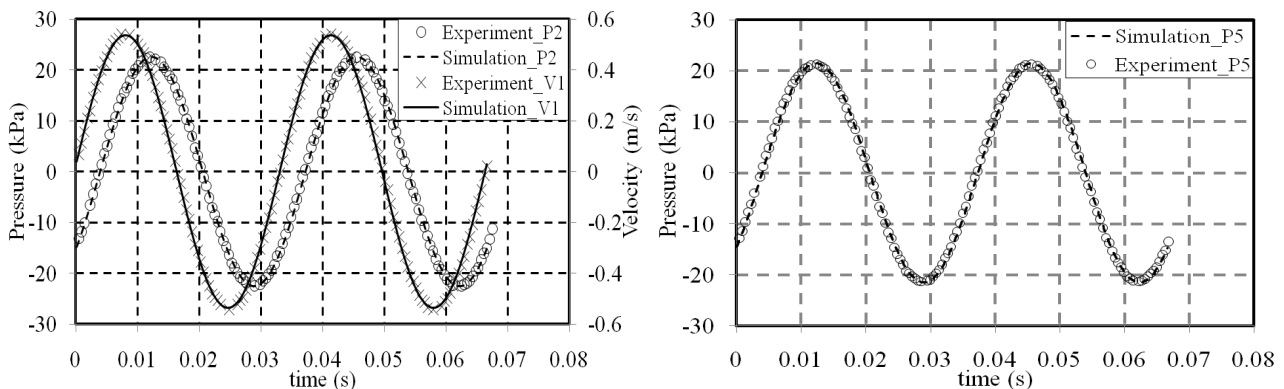


Figure 3: CFD model validation of pressure and velocity at locations before and after the regenerator.

6. RESULTS AND DISCUSSION

Time phasing between pressure and velocity is important in determining the hydrodynamic characteristics of the porous medium such as regenerator. When the pressure and velocity are not in phase, the maximum pressure occurs at a certain phase lag compared to maximum velocity. Hence, the amplitude data will not be accurate enough to represent the friction factor according to eq. (2).

The CFD-assisted model made it possible to compare the phase between pressure drop and velocity in the regenerator. Figure (4) shows that the pressure drop and velocity are in phase within the porous medium region. The result has been checked for all samples, but only one sample case is presented here. Comparing pressure drop with the inlet velocity showed that the inlet velocity was leading the pressure drop by 28° . This

suggests a possible error if the friction factor is calculated based on velocity measured at the inlet location. The implementation of RLC network in the experiment made it possible to control the phase difference between pressure and velocity. As seen from Figure (3) in Section 3. Experimental setup, there existed a phase lag between pressure and velocity at the inlet, and the phase lag was resolved as the flow approached the regenerator. This was made possible by the RLC looping as described in the experimental setup. With this, the flow across the regenerator was controlled via the travelling-wave time phasing and therefore, the friction factor could be calculated using eq. (2) without any ambiguity. The result calculated from the experimentally measured pressure drop and velocity is shown in Figure 5.

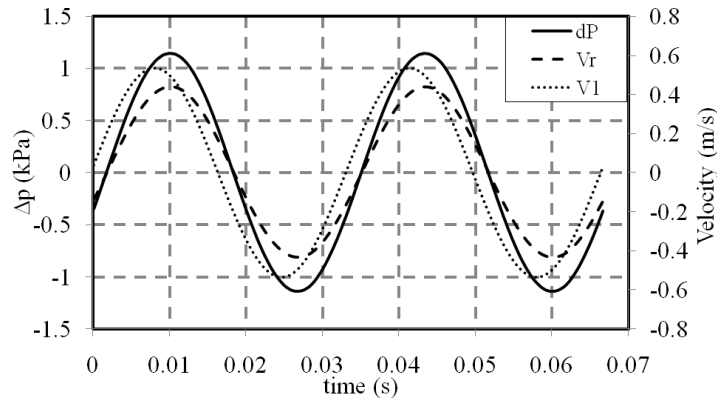


Figure 4: Pressure drop ($\Delta p, dP$) and velocity at two locations; regenerator (V_r) and inlet (V_1)

When modelling the flow in the regenerator, a correct value of permeability is important to make sure that the pressure drop resulted from the simulation matched with the experiment. Permeability is an empirical constant used in the porous medium community to characterize the blockage occurring due to the present of porous media. The results are tabulated in Table 2.

Table 2: CFD-predicted permeability for regenerator investigated

Regenerator mesh number	200	180	94	30
Permeability, K (m^2)	1.766×10^{-10}	1.4907×10^{-10}	1.3435×10^{-9}	1.9×10^{-9}

It is noteworthy that higher regenerator mesh numbers refer to finer meshes. This can be seen in the value of the wire diameter of each sample as listed in Table 1. The permeability coefficient in Table 2 was used to present the CFD-assisted friction factor using eq. (10). The value of permeability is different for each regenerator sample tested. The CFD-assisted results were then compared to the experimental friction factors calculated using eq. (2).

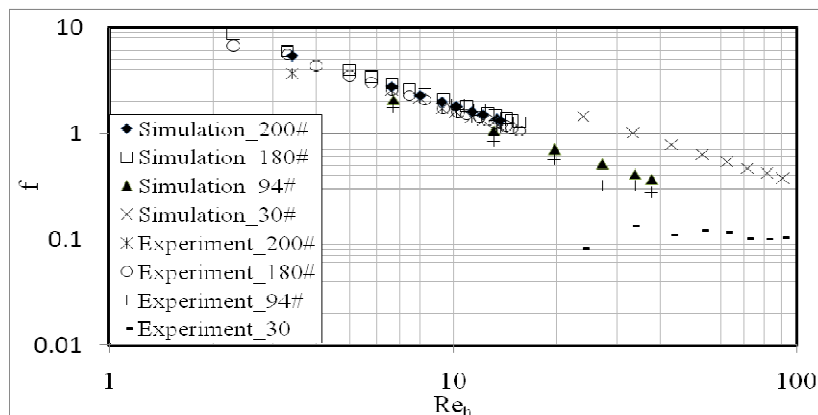


Figure 5: Comparison of friction factors obtained using permeability predictions and experiments.

The friction factor calculated from the equation derived from the CFD model appeared to qualitatively agree with the experimentally calculated value. The quantitative deviation was relatively small except for #30 mesh screen. In the experiment, the velocity was calculated using data collected at the location near the

linear motor. The small deviation could be due to the phase lag between the maximum pressure drop and maximum velocity used in calculating the friction factor.

The permeability obtained from CFD led to overpredictions of the friction factor for #30 mesh screen. The operating velocity recorded in the experiment using the regenerator made out of this mesh was higher compared to other samples tested. When plotted using the representative Reynolds number, this indicated possible inertial effects that should be considered for such meshes. Transient effects were also reported by Hsu (2005) for such a Reynolds number.

7. CONCLUSION

An appropriately defined simulation model of a regenerator, using Fluent, is important as an alternative way of predicting the effects of different regenerator length, material and porosity on the thermoacoustic effect in a travelling-wave system. This paper presents an ongoing research on the regenerator study applied to a thermoacoustic system. A friction factor correlation was derived for the simulation modelled based on the porous medium theory. The simulation results showed a qualitatively good match with the experiments. The reason for quantitative difference was discussed. The phase change between the pressure drop and velocity needs to be carefully determined for an accurate prediction of the friction factor. A significant deviation for the coarse mesh (#30) requires a detailed further analysis to include possible effects of inertia or transient related phenomena. The phase change between pressure and velocity was showed to affect the hydrodynamic characteristics of the regenerator. In thermoacoustics, the phase difference between the pressure and velocity plays an important role. A detailed study of the significance of pressure-velocity phase for the hydrodynamic characteristics of regenerators needs to be undertaken as future work.

8. REFERENCES

- Ashwin TR, Narasimham GSVL, and Jacob S, 2010, CFD analysis of high frequency miniature pulse tube refrigerator for space applications with thermal non-equilibrium model, *Applied Thermal Engineering* 30 152-166
- Bejan A, Dincer I, Lorente S, Miguel AF, and Reis AH, 2004, *Porous and complex flow structures in modern technologies*, Springer. USA. 9p.
- Cha JS, Ghiaasiaan SM, Kirkconnell CS, 2008, Oscillatory flow in microporous media applied in pulse-tube and Stirling-cycle cryocooler regenerators, *Experimental Thermal and Fluid Science* 32 : 1264-1278p.
- Choi S, Nam K, and Jeong S, 2004, Investigation on the pressure drop characteristic of cryocooler regenerators under oscillating flow and pulsating pressure conditions. *Cryogenics* 44 : 203-210.
- Fluent 6.3 User's Guide, Fluent Inc, <<http://www.fluentusers.com/>>.
- Gedeon D, and Wood JG, 1996, *Oscillating-Flow Regenerator Test Rig: Hardware and Theory With Derived Correlations for Screens and Felts*, NASA Contractor Report 198442. NASA Lewis Grantt NAG3-1269.
- Hsu C, 2005, Dynamic Modeling of Convective Heat Transfer in Porous Media, In: Vafai K, *Handbook of Porous Media* 2nd ed, Boca Raton, Taylor and Francis Group, 39-80p.
- Ju Y, Jiang Y, and Zhuo Y, 1998, Experimental study of the oscillating flow characteristics for a regenerator in a pulse tube cryocooler, *Cryogenics* 38: 649-656.
- Nam K, and Jeong S, 2005, Novel flow analysis of regenerator under oscillating flow with pulsating pressure, *Cryogenics* 45: 368-379.
- Nam K, and Jeong S, 2006, Investigation of oscillating flow friction factor for cryocooler regenerator considering cryogenic temperature effect, *Cryogenics* 45: 733-738.
- Swift GW, and Ward WC, 1996, Simple Harmonic Analysis of Regenerators, *Journal of Thermophysics and Heat Transfer*. Vol 10 No.4: 652-662.
- Tao YB, Liu YW, Gao F, Chen XY, and He YL, 2009, Numerical analysis on pressure drop and heat transfer performance of mesh regenerators used in cryocoolers, *Cryogenics* 49: 497-503.
- Yu G, Dai W, and Luo E, 2010, CFD Simulation of 300 Hz thermoacoustic standing wave engine, *Cryogenics* 50: 615-622